Large Temporal Window Near Field Autocorrelator

Contact *alexis.boyle@stfc.ac.uk*

Alexis Boyle, Marco Galimberti

Central Laser Facility, STFC Rutherford Appleton Laboratory
Chilton, Didcot, Oxon. OX11 0QX

Introduction

The synchronized CPA beam 8 (B8) delivered to target area west (TAW) are tunable with respect to beam 7 (B7). Both beams share a stretcher but separate compressors. The standard configuration is to operate B7 at 1ps and detune the B8 compressor to several tens of ps. In the past, a streak camera was used to perform the compressor tuning on B8, but it was not possible to operate this diagnostic on shot. We have developed a large window autocorrelator (AC) capable of measuring pulses of >30ps on shot, with a resolution of 300fs.

Design

All the ACs on Vulcan are standardised, built on 600 x 300 mm breadboards with a common input height and position. The design is kept simple and the AC is performed in the NF. We use pulse front tilt to extend the temporal window of the AC [1, 2]. This allows the AC to be calibrated in the front-end and dropped into place with minimal alignment issues.

Temporal Window

Figure 1 shows the calibration of the large window AC, this was performed using a Ti:Sapphire laser central wavelength 1053nm with a pulse length of 150fs. It was possible to scan the delay arm of the device by almost 70ps from either edge of the temporal window. The AC measured the pulse length of the Ti:Sapphire laser as 300fs suggesting this is the limit of the resolution of the device.
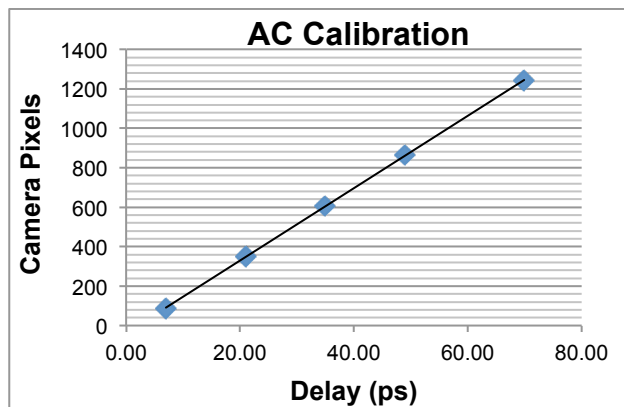

Figure 1: Calibration cure for the AC performed using a 150fs Ti:Sapphire laser.

Results

The AC was installed on B8 in TAW and was used to perform a stretcher tuning curve, shown in figure 2. The AC was run in conjunction with a streak camera using low power shots from Vulcan. Traditionally, the streak camera has been used to perform a coarse scan to suggest where the minimum pulse length is located within 20 mm. The minimum pulse length measurement of the streak camera is documented as 7 ps. A standard AC with a 2 ps window would then be used to locate the minimum pulse length of 1ps. We can clearly see from figure 2, the large window AC has sufficient range to perform the scan over tens of ps. Running this device alongside the streak camera also suggests that the streak camera gives incorrect pulse length measurements in the 7-15ps region.
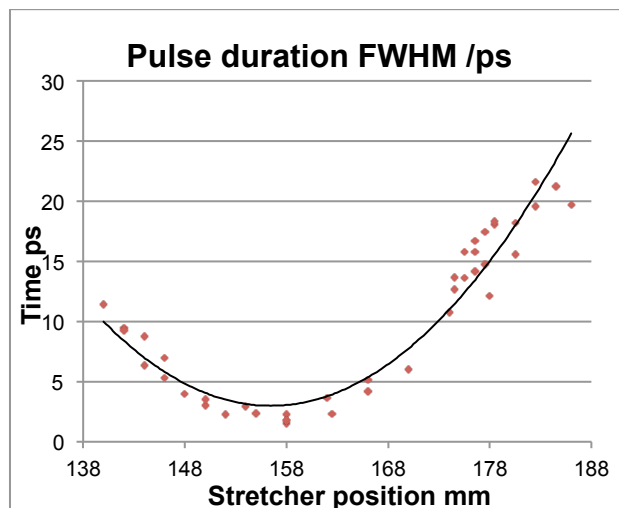

Figure 2: B8 stretcher tuning curve measured using the large window AC.

The device was then commissioned in TAW B8 during an experiment, where the users requested pulse lengths changes between 5 to 20 ps. Figure 3 is a lineout of a 15ps FWHM, full energy (250J) shot. The lineout trace is pretty symmetrical and the jagged profile is caused by intensity variations in the NF profile of the beam.
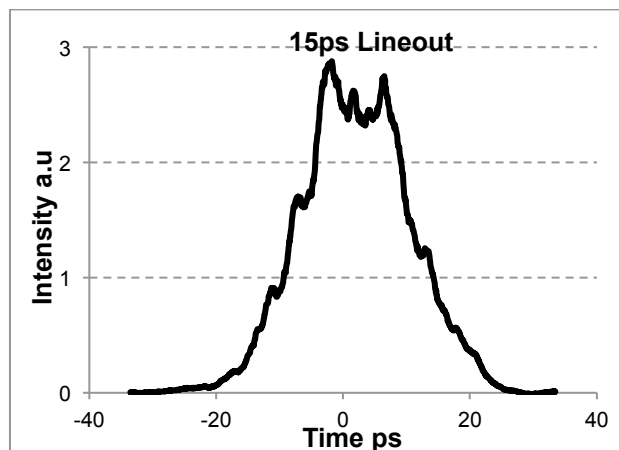

Figure 3: NF AC in TAW beam 7.

Conclusions

Here we present a large temporal window AC of over 70ps and a 300fs resolution. The device has been commissioned and operated on B8 experiments in TAW and produces reliable pulse length measurements in the 1-30ps range.

References

1. J. Janszky, G. Corradi, and R. N. Gyuzalian, Opt. Commun. 23, 293. 1977

2. Uniaxial Single Shot Autocorrelator. Review of Scientific Instruments, Vol 70, No.3. 1999.

Construction of a pump amplifier chain for the 10 J OPCPA beamline

Contact *trevor.winstone@stfc.ac.uk*

TB Winstone, A Boyle, S Chapman, T Critchlow, AJ Frackiewicz, M Galimberti, S Hancock, C Hernandez-Gomez, I Musgrave, DA Pepler, IN Ross, W Shaikh, L Walker,

Central Laser Facility
STFC Rutherford Appleton Laboratory
Chilton, Didcot, Oxon. OX11 0QX

Introduction

The Vulcan 10 PW Upgrade has been designed based on numerical modeling of several different and complex procedures. To ensure that the baseline design is more accurate a test facility has been built to test the first stage of Optical Parametric Chirped Pulse Amplification (OPCPA) gain media. This facility consists of a shaped long pulse oscillator, a rod amplifier, a frequency doubling stage and finally the OPCPA stage. Further we report on the array of diagnostics required to analyse the pump beam as well as the amplified beam.

Shaped Long Pulse Oscillator

A shaped long pulse oscillator[1] has been developed at the Central Laser Facility to enable delivery of a 3 ns flat top pulse both temporally and spatially. The design of this shaped long pulse oscillator is reported elsewhere in this report[2].

Rod Amplifier Chain

A rod amplifier chain is required to amplify the beam from the mJ level at the output of the oscillator to a level of 30 Joules prior to frequency doubling. The Rod Amplifier chain will utilise Quantel[3] rod amplifier heads and power supplies. The amplifiers available to this project are Quantel manufactured heads and power supplies in the form of two 9 mm, one 16 mm, one 25 mm and one 45 mm. All the amplifiers will operate at 2.0 kV of electrical pumping per amplifier.

The architecture of the design is based upon the current Vulcan rod amplifier chain. The Vulcan rod chain design has operated successfully over the past 22 years and would be a good layout to base the rod amplifier section of the pump beamline for the 10 J OPCPA beamline on. However there will be a difference of double passing the 45 mm rod to deliver the required green energy in the pump beam.

At the output of the Shaped Long Pulse oscillator two single pass 9 mm amplifier will be used to boost the energy to the 10's of mJ level before being injected into an air spatial filter. The next two amplifiers will be arranged in a single pass line of 16 mm and 25 mm amplifier. The double passed 45 mm amplifier arrangement will utilize a polarizer, the 45 mm rod amplifier head, a permanent magnet Faraday Rotator and a retro mirror. The beam returning to the polarizer after double passing both the 45 mm rod amplifier and the Faraday will be rejected from the polarizer due to the 90 degree change in polarization and towards the frequency doubling crystal. The focused intensity after the 16 mm rod amplifier is sufficiently high as to breakdown air so vacuum spatial filtering (VSF) is applied.
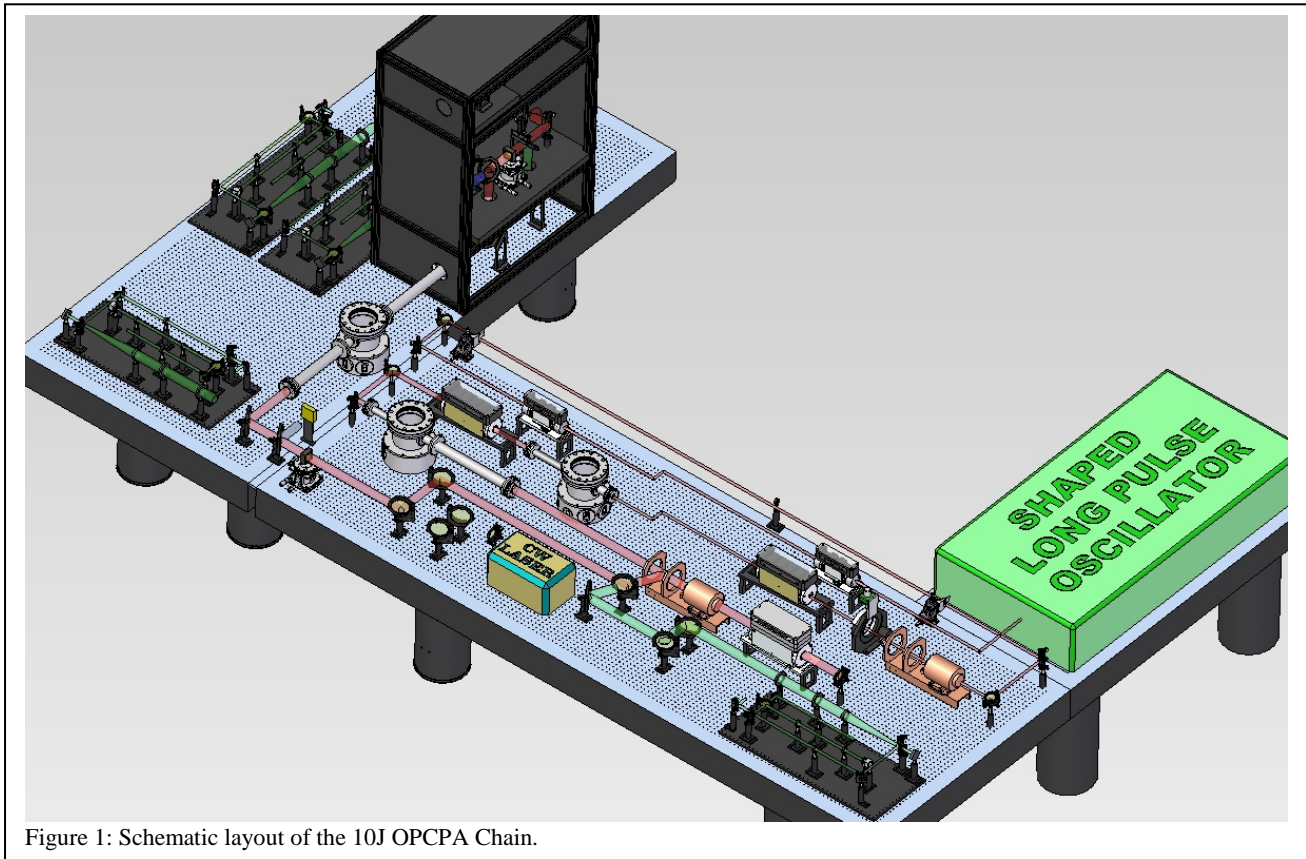

Figure 1: Schematic layout of the 10J OPCPA Chain.

These VSFs will clean the beam and also increase the beam size, hence lowering the beam fluence at the output relative to the input. Between each amplifier stage will be an isolation component, in the form of a Faraday rotator coupled with crossed polarisers to ensure polarization discrimination.

Component	Energy at output	Fluence at output
SLP Oscillator	1.6 mJ	0.02 J/cm^2
First 9	23 mJ	0.23 J/cm2
Second 9	335 mJ	3.13 J/cm^2
16	360 mJ	0.40 J/cm^2
25	2.23 J	0.88 J/cm^2
First pass 45	10.40 J	1.02 J/cm2
Second pass 45	30.07 J	3.38 J/cm^2

With a steadily increasing beam aperture as the pulse passes through the rod amplifier chain the fluence levels are able to be maintained at a reasonable level for the longevity of the system.

Frequency Doubling

The frequency doubling will occur in a Type I Potassium Dihydrogen Phosphate crystal (KDP)[4]. Modelling suggests that the most efficient frequency doubling for the 3 ns pulse from the Type I cut will be from a 20 mm thick crystal. As the KDP Crystal is hydroscopic it will be operated inside a nitrogen cell to reduce water absorption.

Following frequency doubling the 527 nm, 3 ns pulse will pass through an IR mirror at 45 degrees to separate the 527 nm frequency doubled section from the 1053 nm fundamental wavelength. The 1053 nm beam will then be dumped. The 527 nm beam will then be image relayed in a vacuum relay tube before being directed to the Parametric crystal at the same time as the seed pulse from the 10PW Front End[5].

Diagnostics

To enable diagnosis of the pump beamline a diagnostics suite has been designed and built and similar systems will be operated at both then end of the rod chain (1053 nm) and after frequency doubling (527 nm). These diagnostics suites comprise near field and far field cameras, energy monitoring and a fast photo diode for temporal pulse shape measurement.

Conclusions

A system comprising a shaped long pulse oscillator, a Nd:phosphate glass rod amplifier chain and frequency doubling has been built to pump an OPCPA crystal. This will enable better verification of the modeling assumptions of the Vulcan 10 Petawatt upgrade.

References

1   Development, commissioning and experimental delivery of full energy shaped long pulse laser pulses on Vulcan. CLF Annual report 2008-2009 pp 283-285.
2   Modelling and performance of a Regenerative Amplifier Laser Cavity and the rod amplifier chain for the 30J 10 PW CTL pump laser and development of Arbitrary Waveform Generator control software. T Critchlow, W Shaikh. CLF Annual Report 2012-13
3   Quantel SA, 2 bis Avenue du Pacifique, BP23 91 941, Les Ulis CEDEX, France
4   Basic properties of KDP related to the frequency conversion of 1 µm laser radiation, RS Craxton, SD Jacobs, J Rizzo, R Boni; Quantum Electronics, IEEE Journal of (Volume:17, Issue: 9)
5   Optical parametric chirped-pulse amplification source suitable for seeding high-energy systems; Y. Tang et al., Opt. Lett. 33 (20), 2386 (2008).
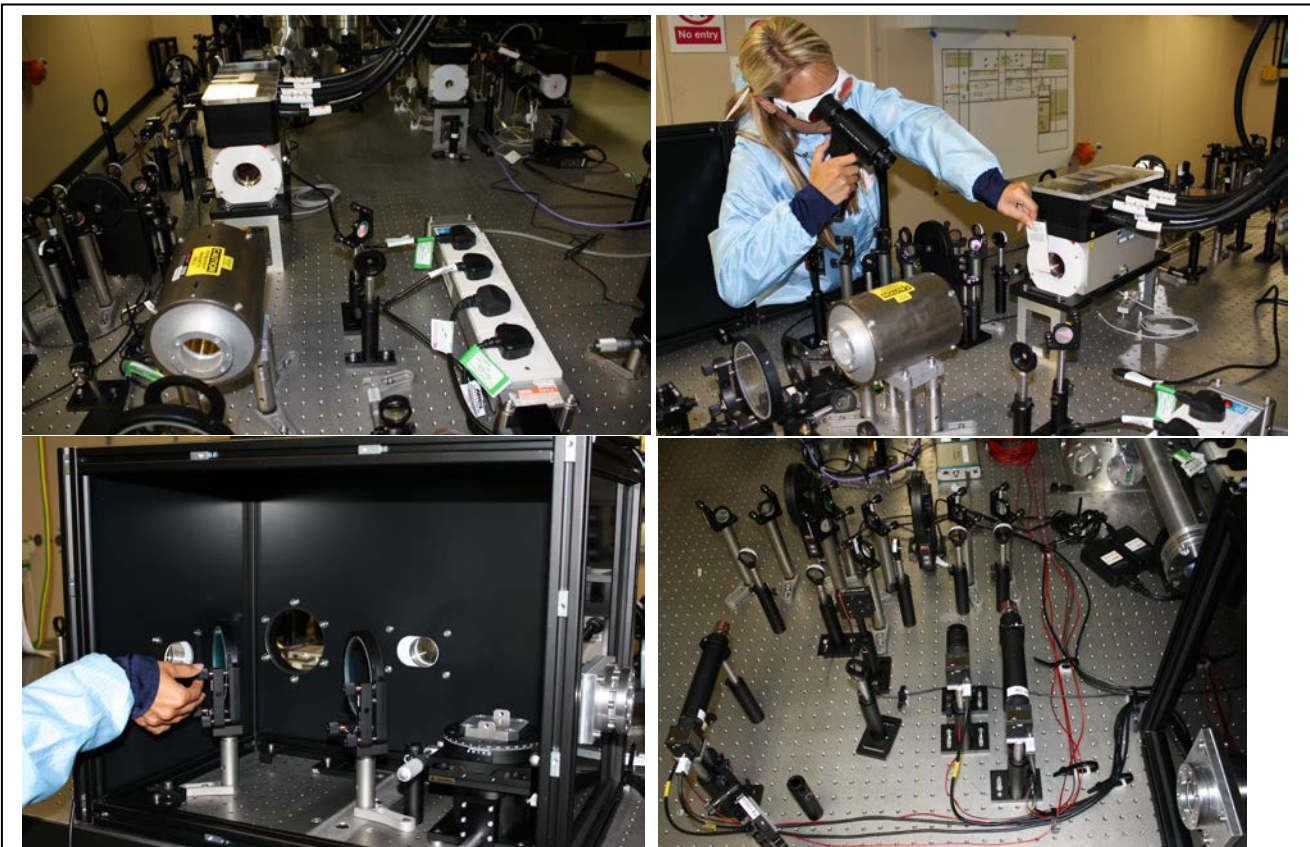
Figure 2; Images of the Pump Laser for the 10 J OPCPA beamline a) View of the complete rod amplifier chain b) Alignment of the double passed 45 mm rod amplifier system with the Faraday Rotator between the first and second passes to reduce likelihood of damage c) Frequency doubling enclosure – the KDP crystal will be installed on the silver pedestal on the right d) Diagnostics assembly showing wide Far Field, Near Field, narrow Far Field, Energy meter and photodiode.

Modelling and performance of a Regenerative Amplifier Laser Cavity and the rod amplifier chain for the 10 J OPCPA pump laser and development of Arbitrary Waveform Generator control software

Contact *tom.critchlow@stfc.ac.uk*

T. Critchlow, W. Shaikh

Central Laser Facility, STFC Rutherford Appleton Laboratory
Chilton, Didcot, Oxon, OX11 0QX

Introduction

Software can be very useful when designing or operating high power laser systems. However, it is often the case that commercial software is not suitable for the task and the creation of an in-house solution is necessary. This report describes software that was developed to aid in the design of the regenerative amplifier cavity as well as a separate piece of software that was developed for control of the temporal shape of the seed pulse for the 10J OPCPA beam-line (Figure 1). We also describe modelling of the rod chain in MIRÓ which is able to predict the energy scaling and pulse shape change as the mJ energy is scaled up to the 30 J level.

The regenerative amplifier was designed as being the mJ seed source for the rod amplifier chain that makes up the 10J OPCPA beam-line.[1] We chose a linear standing wave cavity regenerative amplifier with the gain medium located more than 3ns from the end cavity mirror to avoid pulse distortion[3], seeded from a fibre seed source, which has been temporally shaped by an Arbitrary Waveform Generator (AWG). An 806nm, CW pumped Nd:YLF module acts as the gain medium – this can unfortunately also act as a thermal lens[2] which will affect the stability of the regenerative amplifier.
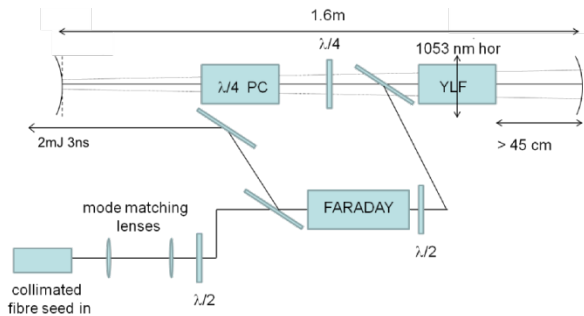

Figure 1: Schematic of regenerative amplifier design.

Resonator Stability

A 'stable' resonator is one in which periodic refocusing of the intracavity beam takes place. In an unstable cavity, the beam size will increase until it eventually grows larger than the size of the end mirrors and escapes.

Certain conditions must be met to produce a stable resonator. The most simple resonator setup consists of a pair of mirrors with radii of curvature R_1 and R_2, separated by a distance L. The stability criteria for such a resonator is [4]

$$0 \leq \left(1 - \frac{L}{R_1}\right)\left(1 - \frac{L}{R_2}\right) \leq 1 \qquad 1$$

A spreadsheet model (Figure 2) of this simple cavity was created in order to lay the foundations for modelling a more complex setup. The model allows the user to enter different values for R_1, R_2, L and λ (the wavelength of the light used,

1053nm for the regen), and it would calculate values for the stability parameter, the radius and position of the beam waist and the radius of the beam at each of the end mirrors. The cavity was also represented graphically by plotting the beam radius

$$w(z) = w_0 \sqrt{1 + \left(\frac{z\lambda}{\pi w_0^2}\right)^2} \qquad 2$$

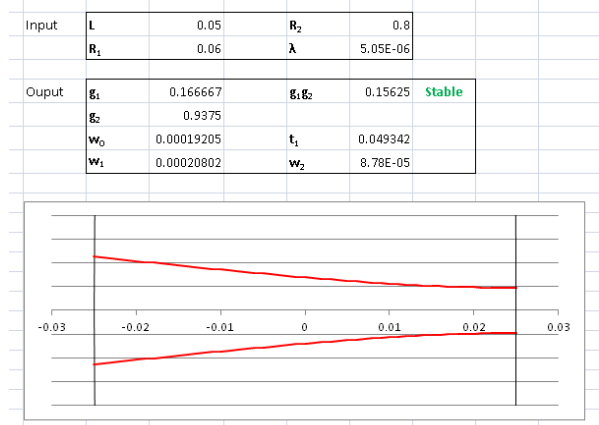where w_0 is the beam waist and the origin of the z-axis is set to its location.[5]

Input				
	L	0.05	R_2	0.8
	R_1	0.06	λ	5.05E-06
Ouput	g_1	0.166667	g_1g_2	0.15625 Stable
	g_2	0.9375		
	w_0	0.00019205	t_1	0.049342
	w_1	0.00020802	w_2	8.78E-05

Figure 2: First spreadsheet model for a simple two mirror cavity.

Ray Transfer Matrix Analysis

In order to model the regenerative amplifier cavity, a technique called ray transfer matrix analysis (also known as ABCD matrix analysis) was used. It involves tracing a path through the system by constructing 2 x 2 matrices that describe the optical effect each component has on the beam. These individual matrices are then multiplied together to give a ray transfer matrix (RTM) for the entire system. Equation 2 shows the RTM for a simple plano-concave resonator of length L where the identity matrix represents reflection from a flat mirror and R_2 is the radius of curvature of the curved mirror.

$$\boldsymbol{M} =$$

$$\begin{bmatrix} 1 & 0 \\ 0 & 1 \end{bmatrix} \begin{bmatrix} 1 & L \\ 0 & 1 \end{bmatrix} \begin{bmatrix} 1 & 0 \\ -\frac{2}{R_2} & 1 \end{bmatrix} \begin{bmatrix} 1 & L \\ 0 & 1 \end{bmatrix} \begin{bmatrix} 1 & 0 \\ 0 & 1 \end{bmatrix}$$

$$= \begin{bmatrix} 1 - \frac{2L}{R_2} & -2(L^2 - LR) \\ -\frac{2}{R_2} & -\frac{2L}{R_2} + 1 \end{bmatrix} \qquad 3$$

It is also possible to calculate resonator stability from ray matrices. To do so, a ray matrix for a round-trip of the cavity must be formulated and from this, we are required to find the

trace of the RTM, which is defined as the sum of the elements on the leading diagonal. This produces new stability criteria

$$0 \leq g \equiv \left| \frac{tr(M)}{2} \right| \leq 1 \qquad\qquad 4$$

Thermal Lensing

The ND:YLF module in the system acts as a 'thermal lens'. Its focusing effects arise from the temperature gradients induced by the beam. The lensing is negative and relatively weak (on the order of 3-5 meters) [6]. The resonator model was rebuilt using Visual Basic and ray matrices (Figure 3). The new model adds the option of including an intracavity (thermal) lens and gives the user control over positioning, focal length and thickness of the lens for flexibility. When the lens is selected, the beam radius at any given point is calculated by finding the RTM for a round-trip to that point and is

$$w^2 = \left(\frac{2\lambda B}{\pi} \right) / \sqrt{4 - (A + D)^2} \qquad\qquad 5$$

where A, B and D are components of the RTM. This new model enabled us to look at and optimize the resonator stability and mode radius for various combinations of cavity length, the radii of curvature of the end mirrors and over the focal length range of the thermal lens.
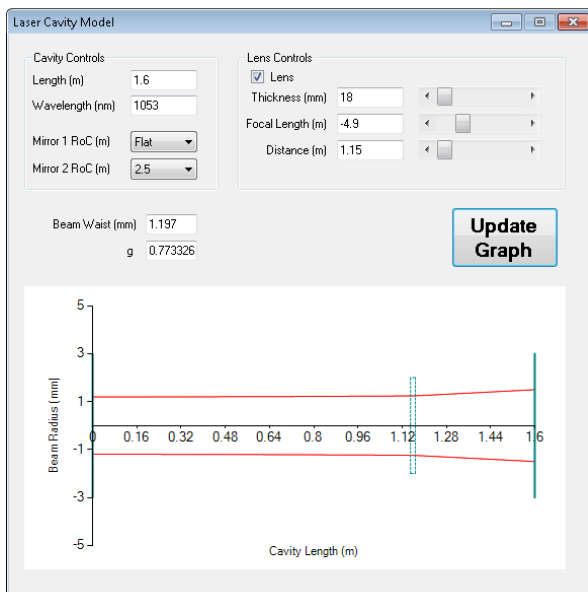

Figure 3: Screenshot of the resonator model including a thermal lens.

The resonator model produces results that match those from a piece of commercial cavity design software, WinLase, but provides a simpler and more accurate representation of the thermal lens. Based on its stability calculations, the length of the regen was shortened from 1.9 m to 1.545 m in an attempt to centre $g = 0.5$ in the middle of the focal length range whilst still ensuring that the laser mode radius was small enough so that the intracavity beam was not diffracted strongly by the gain medium aperture.

The system performed well in recent tests when the picojoule fibre based seed source was suitably telescoped down to match the intracavity mode beam size which was forced towards TEM$_{00}$ by closing down apertures placed close to the cavity end mirrors. There is no evidence of temporal distortion due to pulse overlap with a 3 ns pulse as the YLF crystal was approximately 50 cm from the end mirror. The beam diameter at the gain medium was measured to be 2.2 mm which matches the predicted value to within 5% and is close to the d/π criteria to ensure the near-field beam quality was not unduly affected by the 3mm diameter gain medium (Figure 4). The maximum output energy was close to 1.5 mJ with a RMS stability of 1.255%. This energy stability and the lack of distortion, makes the system far superior to the current shaped long pulse.

AWG Control and Feedback

The regenerative amplifier laser cavity is seeded by a fibre source which passes through an AWG. Vulcan's existing Shaped Long Pulse system also uses an AWG, controlled by software that takes into account the sin^2 transmission dependence on voltage previously described.[7] The AWG in the new setup however is a different model to the one previously used and thus the control software had to be drastically altered. Among the changes was the addition of a shot-to-shot feedback loop as the shape stability of the current shaped long pulse system varies on a day-to-day basis.
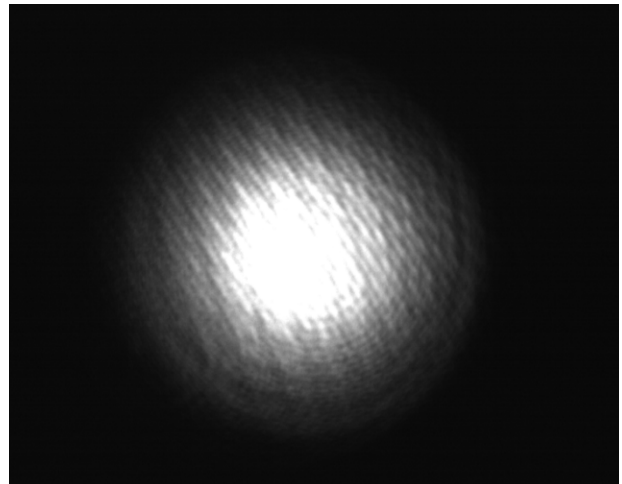

Figure 4: Near-field beam profile obtained by imaging the rod amplifier. (The visible fringes are due to interference that arises in the diagnostics channel)

Whilst not currently complete, the plan is to measure the output pulse shape at a certain point along the system with a diode connected to an oscilloscope. The control software then takes the trace from the oscilloscope and compares it to the desired pulse shape. Then, the most recently sent pulse profile is modified using a dampened correction algorithm and sent back through the system. The corrected pulse can be saved to be used as a jumping-off point for future use.

The initial tests of the feedback loop were promising. The output pulse was multiplied by an arbitrary function to simulate the optical gain of an actual pulse. A trial pulse shape went to a 3ns top hat pulse in less than 10 iterations with the hope of each iteration taking just under 10 seconds. Correction of a sloped or curved pulse was less successful and although this will not be required for the finished system, the algorithm is being worked on to fix this issue.
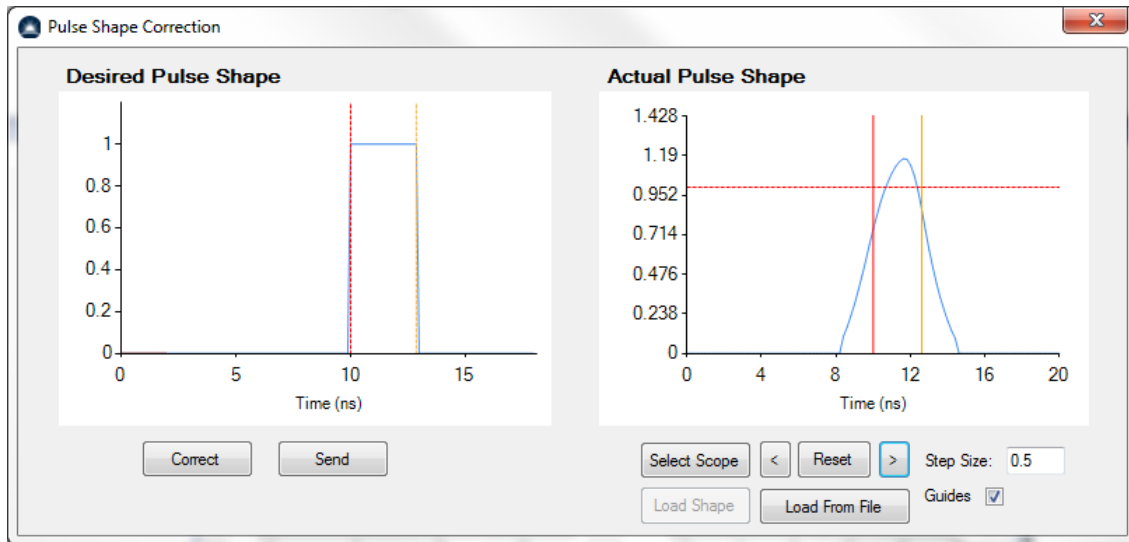
Figure 5: Screenshot of the in progress pulse shape correction program.

MIRÓ Simulation of rod chain performance

The mJ level seed source will need to be amplified to >30J before frequency doubling to provide the OPCPA pump beam at 527nm. This will be achieved by taking the output from the regenerative amplifier and amplifying it in a series of 9mm, 16mm and 25mm rod amplifiers before being double passed in a 45mm amplifier to provide a 38mm diameter output beam.[3] We have modeled this scheme in MIRÓ, showing the typical input pulse profile that will be needed to compensate for gain saturation and provide the super-Gaussian temporal pump profile. The input temporal pump and spatial profile are generated using a 3D analytical expression and adjusted to provide the required output energy, beam diameter, and temporal profile. MIRÓ suggests the optimum doubling crystal thickness to be ~25mm.
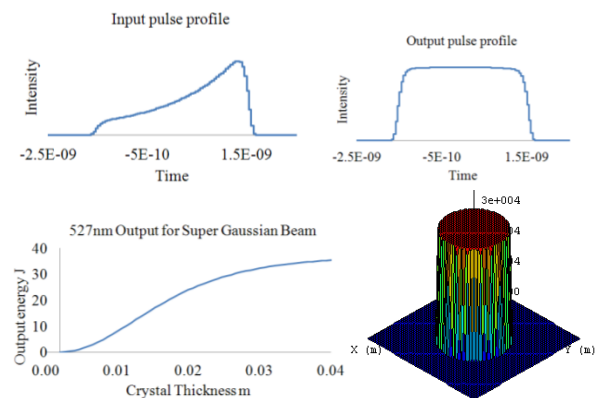

Fig 6: Input and output temporal and spatial pump profile and expected 527nm as a function of KDP crystal thickness.
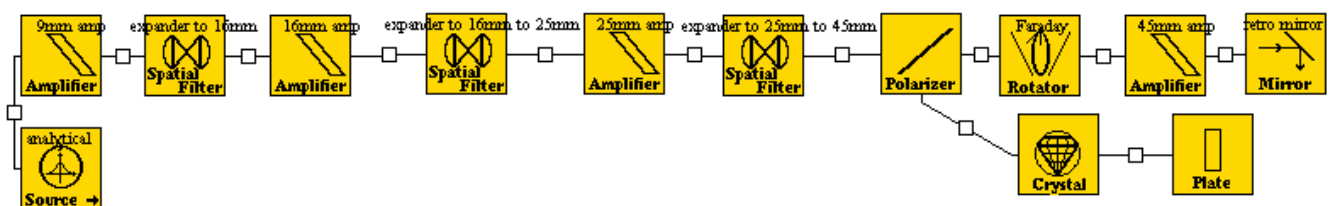

Fig 7: MIRÓ simulation of OPCPA pump architecture.

References

1. T.B. Winstone et al., *Construction of a pump amplifier chain for the 10 J OPCPA beamline,* CLF Annual Report 2012-2013

2. A. Okishev et al., *Highly stable, all solid state Nd:YLF regenerative amplifier,* Applied Optics Vol. 43 No. 33 pp 6180.

3. W. Shaikh et al, *Development of a Pump Laser for a Multi-TW OPCPA Component Test Laboratory,* CLEO 2013 San Jose Convention Centre, 9-14 June 2013.

4. W. Koechner & M. Bass, *Solid-State Lasers*

5. O. Svelto, *Principles of Lasers*, p. 153

6. J. Doster, *RBA YLF Thermal Lensing*, (Northrop Grumman, 2012), Private communication

7. W. Shaikh et al., *Development, commissioning and experimental delivery of full energy chosen shaped long pulse laser pulses at Vulcan,* CLF Annual Report 2008-2009, p.283-285

High Repetition Rate Diagnostics for the Vulcan Laser

Contact *Lukeawalker@hotmail.co.uk*

L. Walker

Central Laser Facility
STFC Rutherford Appleton Laboratory, Chilton, Didcot, Oxon, OX11 0QX

Introduction

In Vulcan there are many parts of the system which receive high repetition rate pulses of frequency 10Hz; these parts of the system are mainly in the Vulcan front end, but certain oscillators can provide pulses which are visible all the way through the rod amplification chain. In order to make better estimations of beam energy and pointing before a shot these pulses must be captured and analysed in real-time; this allows both calculation of the stability of these oscillators as well as real-time data to make decisions with.

In the Vulcan front end there is hardware which instantaneously records the energy of the beam; however there were no pointing monitors, and these energy-meters do not display the energy data in real-time. Because of this, a new piece of software was commissioned which was capable of using uEye® cameras to take energy measurements and to automatically track the position of the beam to warn against pointing errors before they become problematic.

Requirements

The new software was required to capture and display images at a repetition rate of between 2 and 10Hz and to be able to calculate and display a plot of energy (as image intensity) in real-time in order to show recent stability of the laser. Previous investigations have shown that the integral of the intensity of the image has a linear relationship with the energy of the beam, up to the point of saturation [1].

The new software was also required to be able to plot the centroid position as x, y coordinates in real-time, which meant it also needed a fast and reliable centroiding method. This would act as a pointing monitor, to show stability and the current position of the beam. As well as a positional monitor a monitor for the uniformity of the beam – to be measured by finding cross sections along the axes of the beam – was suggested; this would have the benefit of allowing calculation of the beam size based on the full width half maximum of these cross sections.

Final requirements were that it be able to capture images and save them at a speed of 10Hz in order for these images to be analysed later. It was hypothesized that this could be tied in with using a single energy meter in order to calibrate the cameras to produce "real" energy readings; this would provide a calibration gradient and offset in order to convert the integral of the received image into a real energy reading.

Methods

To create the new piece of software an analysis system (Figure 1) was first created; this analysis procedure was intended to be coded into one procedure in Delphi® which could be run at 10Hz. The procedure would first capture an image from the CCD camera, perform some analysis to find and remove any background noise and then integrate the pixel values of the image in order to find the energy of the image. Once this has been done the centroiding algorithm would be performed in order to find the x-, y-coordinates of the centre of the image. Next the image would be displayed with an overlay showing a small cross at the centre of the beam and finally the results of

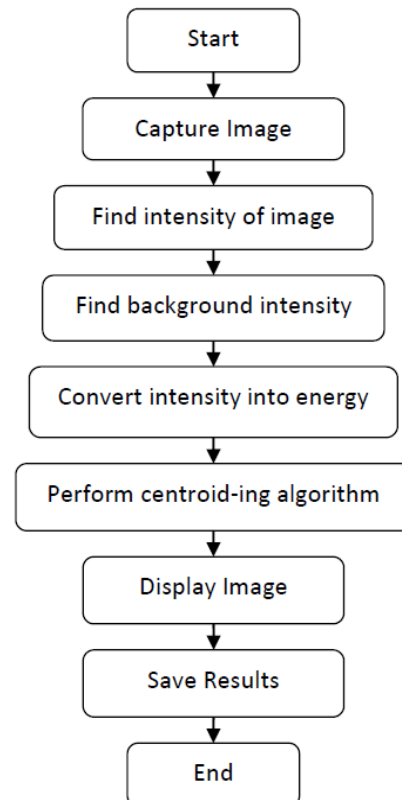the energy and centre calculations would be stored for a short length of time.

Figure 1: Proposed analysis system

In order to perform as required by the specification the analysis procedure had to be able to be performed in less than 500ms; however an analysis time of less than 100ms was aimed for, as this would provide extra time if further real-time analysis needed to be added. In order to perform the analysis at this rate the image needed to be sampled before further operations were done; once the image was sampled in the x- and y-directions this was then integrated to find the energy contained within the image.

Utilising the information from the corners of the image, a background value was then calculated and removed from the image. The background value was calculated to be the average of the lowest intensity corners of the image – preventing the possibility of the beam encompassing one (or more) of these corners and showing a false reading. If any of the corners' average intensity was substantially higher than the other corners, then it was ignored when considering the final background value. Once the background had been removed the "corrected intensity" was calculated and then the calibration factors (intensity to energy) were applied to the "corrected intensity" to get a reading for the energy contained within the image.

Once the energy had been found the centroiding algorithm was run to find the centroid in terms of x- and y- coordinates, with the top left hand corner of the image being referenced as (0, 0). A variety of different centroiding algorithms were investigated, including a method which detects edges to find the centroid of multiple beams upon the camera; however the simplest method was that of Equation (1), which finds the centroid coordinates of the energy distribution across the image [2].

$$M_{ij} = \int_0^Y \int_0^X x^i y^j I(x,y) dx dy \qquad (1)$$

Equation (1) finds the first moment for x (M_{10}) and the first moment for y (M_{01}); which are equivalent to the centroid of the energy distribution. Once these values have been found, they and the energy are plotted on three graphs which show a 10 minute history of these values, allowing an at-a-glance view of the current performance of the oscillator in question.

To find the beam axes the centred second order moments of energy distribution had to be found; these were calculated using Equation (2).

$$\sigma_{ij} = \frac{\int_0^Y \int_0^X I(x,y)(\bar{y}-y)^j (\bar{x}-x)^i dx dy}{\int_0^Y \int_0^X I(x,y) dx dy} \qquad (2)$$

By calculating the second order moment of energy distribution in the x- (σ_{20}), y- (σ_{02}) and xy- (σ_{11}) directions the covariant matrix can be found; the major eigenvector of this matrix can then be calculated to find the x-axis (and by implication the y-axis) of the beam. Once this has been done it is possible to overlay this axis onto the image and move along it, filling an array with the values that lie on this axis. The arrays can then be plotted onto the screen to show the uniformity of the beam, and the FWHMs calculated from these arrays.

Final Software

The final piece of software was entitled "Measure Energy and Plot" (MEAP) (Figure 2); capable of performing all the tasks laid out by the brief, this has quickly evolved into a useful piece of diagnostic software.
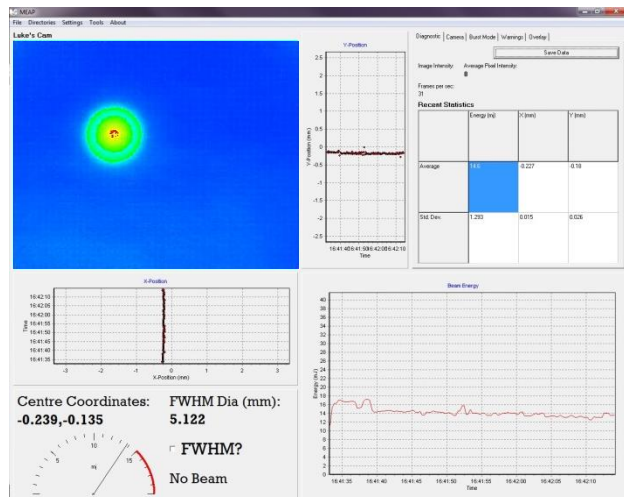

Figure 2: Measure Energy and Plot

In figure 2 a laser beam is being viewed in false colour mode, which allows the user to see more clearly hot spots and saturation in the beam. A further contour image display mode that shows the beam as a contour map is included, and the traditional greyscale image can be viewed. Graphs of energy, x and y position against time can also be seen, these display the history of these variables for 10 minutes. Statistics such as average and standard deviation can are regularly calculated for the previous 10 minutes and are displayed in the table. Other direct diagnostic feedback tools with MEAP include the ability to view a cross section of the energy profile of the beam and the

ability to find the diameter of the beam, based on a number of different measurements including the FWHMs, which is the default.

As well as being able to measure a beam, MEAP is also able to recognise if a beam is not present; this feature enables the possibility of a warning if an expected beam is not present. This also prevents the recording of unnecessary data, which saves time and memory space.

MEAP can save images at a repetition of rate of 10Hz, and is also capable of instantaneously saving the previous 10 minutes of data in a single button press. Alternatively MEAP is able to save data over longer periods of time: a feature enables regular saving to a daily data file which can be used to show data over the period of a day; or data files can be compounded to view data over longer periods of time.

MEAP also included functionality to communicate with a variety of programs over a network via TCP/IP. This enables the combination of diagnostic feedback with active control systems or separate servers to compound and display data in a centralised location.

Conclusions

The final software has been used to monitor stability in some of the laser oscillators over long periods of time; this has been extremely successful in identifying sources of potential instability.

MEAP has been used to capture data from places within the Vulcan rod chain, this data has been used to get a clearer idea of the stability of the Vulcan laser for various oscillators. MEAP is also installed on some PCs to act as a permanent beam monitor: the real-time graph of energy is a useful tool for use in Vulcan operations.

MEAP has also been used to trial an energy control system; the TCP/IP communication function allows data recently taken to be received by other programs and used to actively control the energy level of the beam.

References

1. N Stuart, 2010. *Physics with Industrial Experience Final Report*. Department of Physics, University of Bristol [Accessed on 02/07/2013]

2. International Standards Office, 2005. *ISO 11146, Lasers and laser-related equipment – Test methods for laser beam widths, divergence angles and beam propagation ratios.* Geneva: ISO [Accessed on 01/07/2013]